doi: 10.12029/gc20200401

陈超, 苑金玲, 郭盼, 黎方云, 孔令耀, 杨金香, 毛新武. 2020. 扬子陆块~2.0 Ga的区域变质事件对南北黄陵古元古代差异演化的启示[J]. 中国地质, 47(4): 899−913.

Chen Chao, Yuan Jinling, Guo Pan, Li Fangyun, Kong Lingyao, Yang Jinxiang, Mao Xinwu. 2020. ~2.0 Ga regional metamorphic event in Yangtze block and its heuristic significance to the geological differences evolutionary between north and south Huangling[J]. Geology in China, 47(4):899−913(in Chinese with English abstract).

扬子陆块~2.0 Ga的区域变质事件对南北黄陵古元古代差异演化的启示

陈超[1,2,3], 苑金玲[4], 郭盼[1], 黎方云[1], 孔令耀[1], 杨金香[1], 毛新武[1]

(1. 湖北省地质调查院,湖北 武汉 430034;2. 中国地质大学(武汉)地球科学学院,湖北 武汉 430074;3.湖北省地质勘查工程技术研究中心,湖北 武汉 430034;4.湖北省地质科学研究院,湖北 武汉 430034)

提要:扬子陆核黄陵地区发育较为完整的太古宙—古元古代片麻岩、表壳岩组合(即崆岭杂岩),前人调查研究认为南北黄陵$Ar-Pt_1$具有一致的物质组成和地质演化过程。笔者分别对南北黄陵太古宙花岗质片麻岩进行锆石年代学研究发现,北黄陵2件样品(HL013−1、HL013−2)均存在大量锆石发育岩浆核−变质边结构,都获得~2.8 Ga原岩结晶年龄和~2.0 Ga变质年龄;而南黄陵1件样品(HL005−3)以具振荡环带结构的岩浆锆石为主,仅获得~2.9 Ga原岩结晶年龄。结合前人研究成果发现,~2.0 Ga的变质年龄在北黄陵太古宙—古元古代的花岗片麻岩、表壳岩中广泛发育,而在南黄陵相似建造中均未获得,一定程度上说明北黄陵地区广泛遭受~2.0 Ga的区域变质作用而南黄陵不发育,南北黄陵在古元古代可能处在不同地块或者同一地块不同部位。2.1~1.6 Ga的构造岩浆事件的分布特点说明扬子陆块可能存在多条古元古代造山带,扬子陆块古元古代以多块体拼贴为特点,广泛记录2.1~1.6 Ga的构造岩浆事件说明扬子陆块是全球哥伦比亚超大陆的重要组成部分。

关 键 词:扬子陆块;崆岭杂岩;古元古代;~2.0 Ga变质事件;哥伦比亚超大陆;地质调查工程

中图分类号:P618.51 **文献标志码**:A **文章编号**:1000−3657(2020)04−0899−15

~2.0 Ga regional metamorphic event in Yangtze block and its heuristic significance to the geological differences evolutionary between north and south Huangling

CHEN Chao[1, 2, 3], YUAN Jinling[4], GUO Pan[1], LI Fangyun[1], KONG Lingyao[1], YANG Jinxiang[1], MAO Xinwu[1]

(1. *Hubei Geological Survey, Wuhan* 430034*, Hubei, China;* 2. *Faculty of Earth Sciences, China University of Geoscieces, Wuhan* 430074*, Hubei, China;*3.*Hubei Research Center of Geological Exploration and Engineering Technology,Wuhan* 430034*,Hubei , China*;4. *Hubei Institute of Geosciences, Wuhan* 430034*, Hubei, China)*

Abstract: A set of integrated Archean−Paleoproterozoic gneisses and supracrustal rocks are exposed in Huangling area, Yangtze

收稿日期:2019−05−05;**改回日期**:2019−12−26

基金项目:湖北省地质局项目(KJ2019−2)、中国地质调查局项目(DD20190370)资助。

作者简介:陈超,男,1987年生,博士生,主要从事基础地质调查与研究工作;E−mail:410104436@qq.com。

continental nucleus, and are named Kongling Complex. Previous research shows that north and south Huangling had the same material composition and geological evolution process in Ar−Pt_1. Zircon dating studies of Archean granitic gneiss from the north and the south of Huangling respectively show that two samples (HL013−1 and HL013−2) from the north huangling contain a large amount of zircons with the development of core−rim structure, and have protolith age of ~2.8 Ga and metamorphic age of ~2.0 Ga, whereas one sample (HL005−3) from south Huangling mainly contains magmatic zircons with oscillatory zones, and has a crystallization age of ~2.9 Ga only. Combined with previous research results, the authors found that the metamorphic age of ~2.0 Ga was widely obtained in the Archean−Paleoproterozoic granitic gneiss and supracrustal rocks from north Huangling, but was not obtained in the similar structures from south Huangling. This is probably due to the fact that north Hangling had widely developed ~2.0 Ga regional metamorphism but south Huangling had not, and they were probably in different massifs or different parts of the same massif in Paleoproterozoic period. The spatial distribution characteristics of 2.1−1.6 Ga tectono−magmatic events in Yangtze block indicate that there may have existed multiple Paleoproterozoic orogenic belts, characterized by the evolution of multi−block collage in Paleoproterozoic. The extensive records of 2.1−1.6 Ga tectono−magmatic events indicate that the Yangtze block is an important part of the global Columbian supercontinent.

Key words: Yangtze block; Kongling complex; Paleoproterozoic period; ~2.0 Ga metamorphic event; Columbia supercontinent; geological survey engineering

About the first author: CHEN Chao, male, born in 1987, doctor candidate, engages in basic geological survey and research; E−mail: 410104436@qq.com.

Fund support: Supported by the projects of Hubei Geological Bureau (No.KJ2019−2) and China Geological Survey(No.DD20190370).

1 引 言

湖北宜昌黄陵地区发育较为完整的前南华纪基底建造，区内最老的物质可以追溯到古太古代（约3.45 Ga）(Guo et al., 2014)，是扬子陆块古老陆核的重要窗口之一，对研究扬子陆块乃至全球大陆早期形成演化过程、超大陆旋回等具有重要意义。黄陵地区大体以雾渡河一带为界南北表现出较大差异，北黄陵主要出露太古宙—古元古代花岗片麻岩、表壳岩，而南黄陵以新元古代花岗质片麻岩为主，少量太古宙花岗质片麻岩和古元古代表壳岩。近年来，以彭松柏教授为主的研究团队先后在南、北黄陵有限范围内分别厘定出庙湾蛇绿混杂岩（1.14~0.97 Ga）(彭松柏等, 2010; Jiang et al., 2012; Peng et al., 2012a; Jiang et al., 2016; Deng et al., 2017)、水月寺蛇绿混杂岩（2.15~2.12 Ga）(Han et al., 2017, 2018)，分别代表罗迪尼亚超大陆、哥伦比亚超大陆汇聚事件在扬子陆块的响应。从基本的物质结构特点上看，南北黄陵表现出明显的差异，但除去南黄陵新元古代侵入岩和庙湾蛇绿混杂岩，二者表现出较强的相似性(Gao et al., 2011)。另外，Han et al. (2017, 2018)对北黄陵水月寺蛇绿混杂岩进行锆石年代学研究时发现~2.1 Ga的蛇绿岩经历了~2.0 Ga的区域变质作用，且该变质事件在北黄陵太古宙—古元古代其他建造中广泛纪录(Yin et al., 2013; Chen et al., 2013a; Guo et al., 2015; Li et al., 2016)，但在南黄陵近同期建造中均未获得该变质年龄(Gao et al., 2011; Li et al., 2018)。本文以南北黄陵太古宙片麻岩为切入点，以锆石U−Pb测年为关键手段，结合前人调查研究成果，探讨南北黄陵古元古代演化的差异，进而根据古元古代构造−岩浆作用在扬子陆块分布情况，初步探讨扬子陆块古元古代地质演化特点，及其与哥伦比亚超大陆汇聚过程的关联性。

2 区域地质特征

研究区位于扬子地块北部，区内主要出露扬子地块前南华纪基底，周围被南华系及其上盖层角度不整合掩盖（图1），习惯上称其为“黄陵背斜”。黄陵地区因发育太古宙—古元古代崆岭杂岩而成为前寒武纪研究的热点，崆岭杂岩主要分布于雾渡河断裂以北的北黄陵地区，主要由结晶基底片麻岩和表壳岩系组成，并被古元古代末期（约1.8 Ga）圈椅埫A型花岗岩侵入(Xiong et al., 2009; Peng et al., 2012b)。其中结晶基底片麻岩包括闪长质、英云闪长质、奥长花岗质、花岗闪长质片麻岩（DTTG）和花岗质片麻岩(高山等, 2001)，根据现有研究其形成时间可能跨度到3.45~2.00 Ga(Gao et al., 2011; Chen

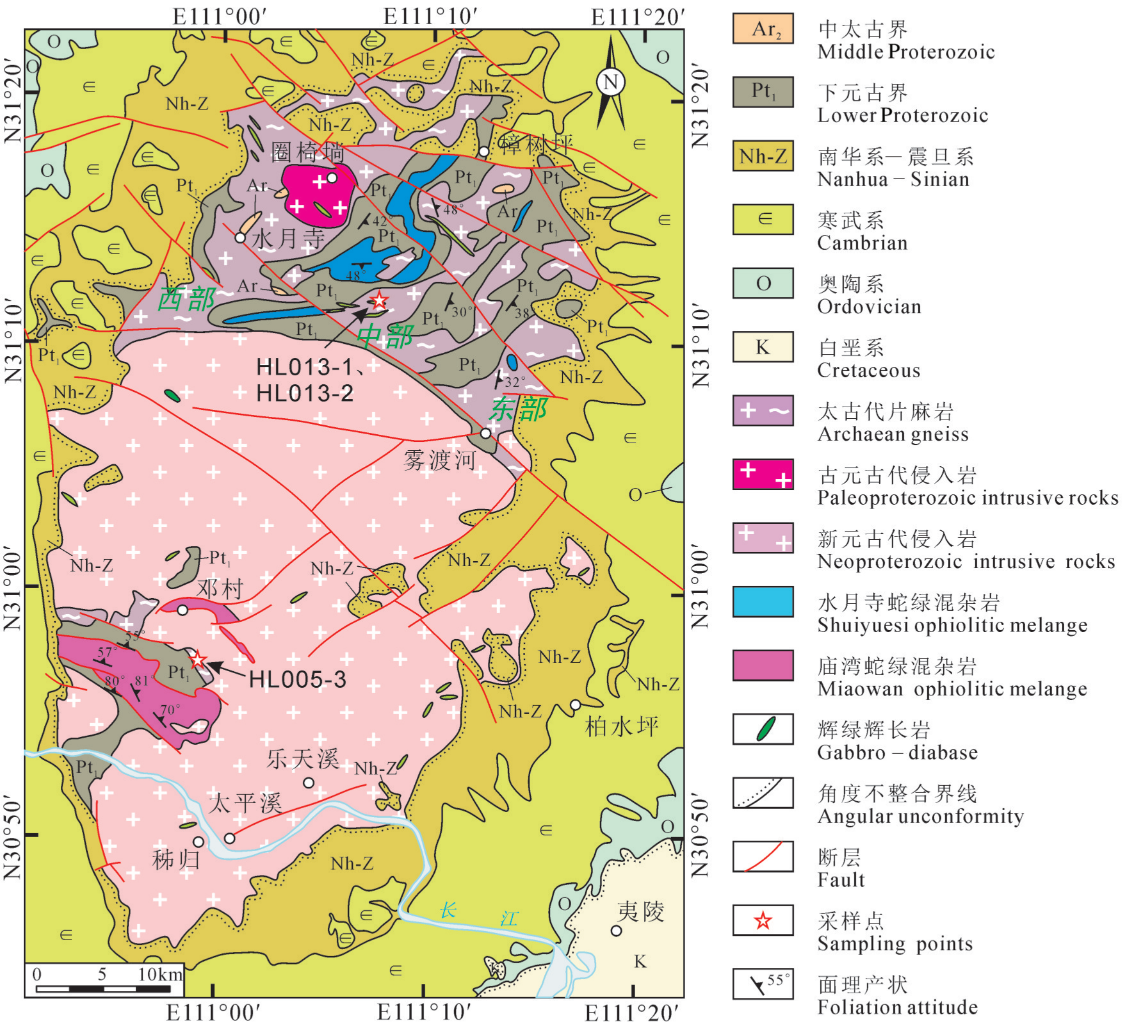

图1 黄陵地区地质简图

Fig.1 Geological sketch map of the Huangling area

et al., 2013a; Guo et al., 2014, 2015);表壳岩系包括两套岩石组合❶:①中太古界野马洞组,为一套混合岩化的斜长角闪岩、黑云斜长变粒岩、黑云角闪斜长片麻岩、石英片岩、角闪片岩和黑云片岩,达到角闪岩相变质,多呈包体形式赋存于太古宙片麻岩中,魏君奇等(2012)从中获得了3.0 Ga的成岩年龄和2.7 Ga、2.5 Ga的变质年龄;②古元古界黄凉河组,为一套孔兹岩系,主要由富铝片岩—片麻岩及石榴夕线石英岩、长英质粒岩、斜长角闪岩、大理岩和钙镁硅酸盐岩4类组成,其形成时间大体可以限定为2.1~2.0 Ga,并广泛遭受~2.0 Ga的变质作用(Zhang et al., 2006; Yin et al., 2013; Li et al., 2016; 邱啸飞等, 2016, 2017)。此外,沿着北黄陵中部北东−南西向出露的变镁铁质—超镁铁质岩组合可能代表一套蛇绿混杂岩——水月寺蛇绿混杂岩,其形成背景可能与古元古代哥伦比亚超大陆汇聚过程有关(Han et al., 2017, 2018)。南黄陵以大面积出露新元古代(863~794 Ma)侵入岩为显著特点(凌文黎等, 2006; Zhang et al., 2009; Zhao et al., 2010a; Wei et al., 2012; Zhao et al., 2013; Wu et al., 2016),仅在邓村—秭归一带存在少量太古代片麻岩和古元古代表壳岩(Gao et al., 2011; Li et al., 2018),以及近东西向展布的中—新元古代庙湾蛇绿混杂岩(Peng et al., 2012a; Jiang et al., 2016; Deng et al., 2017)。

3 样品特征和分析方法

3.1 样品特征

北黄陵2件片麻岩样品采自水月寺蛇绿岩东侧

的“小坪杂岩”(采样位置见图1),1∶25万荆门市幅显示其形成于新元古代❶。小坪杂岩主要由花岗闪长质片麻岩、二长花岗质片麻岩、英云闪长质片麻岩等组成,不同岩性之间相互穿插(图2a),片麻理较为发育(图2b)。花岗闪长质片麻岩(HL013-1)具鳞片花岗变晶结构,片麻状构造,主要由石英(35%)、斜长石(43%)、钾长石(15%)组成,次要矿物为黑云母,副矿物为锆石。石英呈粒状、他形粒状,粒径0.5~1.8 mm,波状消光;斜长石呈板粒状,粒径0.7~2.5 mm,发育细密聚片双晶;钾长石呈粒状或他形粒状,粒径0.5~1.0 mm,解理发育,双晶少见,内部常含石英包体;黑云母呈鳞片状,粒径0.3~0.6 mm,断续弱定向性排列,构成岩石弱片麻理;锆石少见,呈半自形柱状,粒径0.05 mm(图2c)。斑状钾长花岗质片麻岩(HL013-2)具有变余斑状结构,块状构造,斑晶为钾长石(4%)及石英(6%),基质为石英(28%)、钾长石(50%)、斜长石(10%),次要矿物为黑云母,副矿物为磁铁矿。钾长石斑晶呈板粒状,粒径0.4~1.0 mm,可见条纹结构及隐约格子双晶;石英斑晶呈粒状,粒径0.3~0.5 mm,内部常有细粒化现象。基质中以钾长石为主体,呈变晶粒状,粒径0.06~0.15 mm,解理发育;石英变晶粒状,粒径0.1 mm,与长石类矿物彼此镶嵌排列;斜长石呈变晶粒状,粒径0.1 mm,可见细密聚片双晶;磁铁矿粒状,粒径0.1~0.25 mm,零星分布(图2d)。

南黄陵1件片麻岩样品采自邓村南侧的山顶公路边,主体为一套二长花岗质片麻岩,片麻理产状230°~250°∠60°~75°,局部可见两期岩脉侵位,早期弱变质辉绿岩脉斜切片麻理,晚期未变质钾长花岗岩脉切穿片麻理和早期辉绿岩脉(图2e)。黑云二长花岗质片麻岩(HL005-3)具鳞片花岗变晶结构,片麻状构造,主要矿物为石英(35%)、斜长石(36%)、钾长石(30%),次要矿物为黑云母。斜长石呈粒状,粒径0.2~0.6 mm,常见细密聚片双晶,解理发育,表面轻度绢云母化;钾长石嵌晶粒状,粒径0.2~0.7 mm,解理发育,双晶少见;石英嵌晶粒状,与长石类矿物镶嵌排列,粒径0.2~0.7 mm;黑云母呈棕褐色片状,粒径0.2~0.5 mm,总体呈断续定向性排列,构成岩石片麻理(图2f)。

3.2 分析方法

锆石挑选、制靶、反射光、透射光和阴极发光拍照在南京宏创地质勘查技术服务有限公司完成,将样品粉碎到0.180~0.154 mm(80~100目),然后利用常规的浮选和电磁法分离出锆石,在双目镜下挑选出晶型较好的锆石制靶,阴极发光(CL)采用TESCAN MIRA3场发射扫描电镜和TESCAN公司阴极发光探头进行锆石内部结构分析研究。LA-ICP-MS锆石U-Th-Pb同位素和微量元素微区分析在湖北省地质试验测试中心完成,测试仪器采用美国Coherent Inc公司生产的GeoLasPro全自动版193 nm ArF准分子激光剥蚀系统(LA)和美国Agilent公司生产的7700X型电感耦合等离子质谱仪(ICP-MS)联用构成的激光剥蚀电感耦合等离子体质谱分析系统(LA-ICP-MS),激光束斑直径为32 μm,用He作为剥蚀物质的载气,哈佛大学标准锆石91500作为外标,GJ-1或者Plešovic为监控标样,实验仪器参数设置与中国地质大学(武汉)地质过程与矿产资源国家重点实验室仪器一致(周亮亮等, 2017)。采用ICPMSDataCal (V10.1)软件对测试结果进行分析(Liu et al., 2009),所得的数据用Isoplot 3.0程序进行谐和图绘制和加权平均年龄计算(Ludwig, 2003)。

4 锆石U-Pb测年结果

北黄陵花岗闪长质片麻岩(HL013-1)和斑状钾长花岗质片麻岩(HL013-2)中锆石大部分自形程度较高,粒径一般大于100 μm,锆石被改造强烈,部分锆石存在明显的岩浆核-变质边结构(图3),2件样品共67个分析点中(表1),除HL013-2-17分析点误差较大舍弃,44个岩浆核分析点Th/U比值为0.11~1.12,22个变质边分析点Th/U比值为0.05~0.21,二者表现出显著不同的特点(图4a)。花岗闪长质片麻岩(HL013-1)23个岩浆核分析点产生上交点年龄为(2874±35) Ma (MSWD=0.44),13个变质边分析点产生上交点年龄为(2037±26) Ma (MSWD=1.6)(图4b);斑状钾长花岗质片麻岩(HL013-2)21个岩浆核分析点产生上交点年龄为(2852±40) Ma (MSWD=1.9),9个变质边分析点产生上交点年龄为(2005±31) Ma (MSWD=1.8)(图4c)。2件样品测试结果基本一致,岩浆核产生的上交点年龄为原岩成岩年龄(~2.8 Ga),变质边产生的年龄为变质年龄(~2.0 Ga)。从锆石的谐和年龄图可以

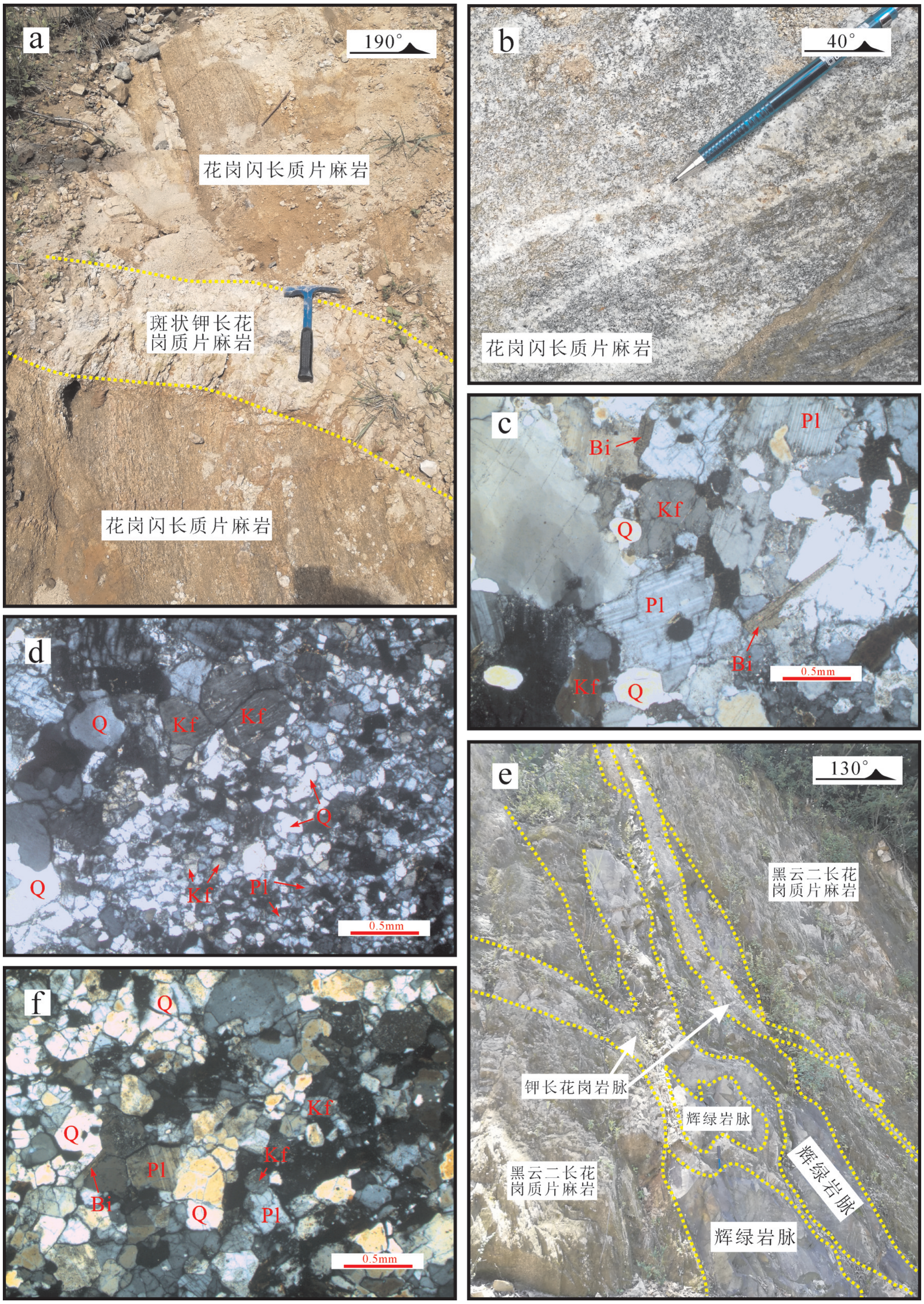

图2 黄陵地区太古宙片麻岩野外及镜下照片

Fig.2 Field photographs and photomicrographs for the Archaean gneisses from the Huangling area

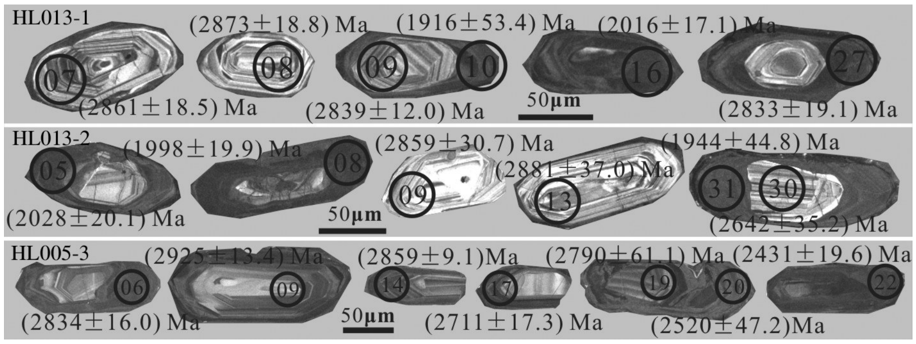

图3 黄陵片麻岩HL013−1、HL013−2、HL005−3典型锆石阴极发光图(CL)
Fig.3 Typical Cathodoluminescence (CL) images of zircons from the gneisses (HL013−1, HL013−2, HL005−3) in the Huangling area

发现,两件样品成岩固结之后,可能至少经历了两次较为强烈的构造热事件改造。

南黄陵黑云二长花岗质片麻岩(HL005−3)中锆石以发育较好的振荡环带结构为主,仅部分发育弱的变质边(图3),42个分析点Th/U比值与北黄陵2件片麻岩样品存在较大不同,0.03~1.05均匀分布,产生上交点年龄为(2921±11) Ma (MSWD=2.3)(图4a、d),代表黑云二长花岗质片麻岩原岩的成岩年龄。南黄陵太古代片麻岩锆石虽然也存在改造的痕迹(有变质边、部分Th/U比值<0.1),但42个分析点一致产生一个上交点年龄~2.9 Ga、下交点年龄317 Ma(下交点年龄在这里无意义),说明其与北黄陵两件样品不同,仅经历一次构造热事件改造。从中也未获得~2.0 Ga的变质年龄,说明~2.0 Ga的变质事件对南黄陵影响有限。

5 讨　论

5.1 南北黄陵古元古代差异演化

对比南北黄陵太古宙崆岭杂岩,北黄陵发现的最早的岩石为~3.45 Ga花岗质片麻岩(Guo et al., 2014),2.6~3.3 Ga构造岩浆事件在北黄陵较为发育(Qiu et al., 2000; Jiao et al., 2009; Gao et al., 2011; Chen et al., 2013a; Guo et al., 2014, 2015; Li et al., 2016)。而南黄陵最老仅获得~2.9 Ga的TTG片麻岩、混合岩(Gao et al., 2011; Li et al., 2018),这与笔者获得的~2.9 Ga二长花岗质片麻岩为同一期产物。此外,南黄陵未发现其他太古宙实体建造,但在南黄陵古元古代变沉积岩中保留了2.6~3.5 Ga的碎屑锆石,说明太古宙南北黄陵存在一定相关性(Gao et al., 2011; Li et al., 2018)。

古元古代,北黄陵先后经历了~2.4 Ga的岩浆侵位(Guo et al., 2015)、2.15~2.0 Ga的俯冲−碰撞过程(Han et al., 2017, 2018; Li et al., 2019)和沉积事件(Yin et al., 2013; Li et al., 2016; 邱啸飞等, 2016, 2017)、~2.0 Ga的变质作用(Zhang et al., 2006; Wu et al., 2009; Yin et al., 2013; Chen et al., 2013a; Li et al., 2016; Han et al., 2017; 邱啸飞等, 2017, 2019)以及~1.8 Ga区域伸展事件(Xiong et al., 2009; Peng et al., 2012b; 赵敏, 2013);而南黄陵仅发现了与北黄陵类似的古元古代孔兹岩系❷(具体沉积时间暂无同位素年龄限制)和~1.76 Ga的A型花岗岩及其中2.4 Ga、2.0 Ga的捕获锆石(Li et al., 2018),分别代表南黄陵对应的沉积事件和伸展过程(图5)。不难发现,南、北黄陵古元古代存在一个重要差异:北黄陵太古宙—古元古代的片麻岩、表壳岩系(包括水月寺蛇绿混杂岩中)均记录了~2.0 Ga的变质事件(Han et al., 2017; 邱啸飞等, 2017, 2019),而南黄陵太古宙片麻岩、古元古代表壳岩中均未获得该变质年龄(Gao et al., 2011; Li et al., 2018)。这一定程度上说明南黄陵可能未经历~2.0 Ga区域变质作用,此时的南、北黄陵可能处于不同的大地构造环境,也许是不同地块,或者是同一地块不同位置。

北黄陵根据物质建造和变形变质特点大体可分为东、中、西三部分(图1)(Li et al., 2018),南黄陵与北黄陵西部均以~2.9 Ga的片麻岩为主、经历2.6~2.7 Ga的再造、基本未遭受~2.0 Ga的变质作用、但同发育~1.8 Ga的A型花岗岩(李一鹤, 2016; Li et al., 2018; Han et al., 2019),二者表现出较强的亲缘性。北黄陵中、东部处于活跃的造山带环境,发育经典造山带较为完整的蛇绿岩、弧岩浆岩、沉积岩、

表1 片麻岩HL013−1、HL013−2、HL005−3 LA−ICP−MS测年结果

Table 1 LA−ICP−MS dating data for the gneisses HL013−1, HL013−2 and HL005−3

分析	含量/10^{-6}			Th/U	比值						年龄/Ma					
点号	Pb	Th	U		^{207}Pb/^{206}Pb	1σ	^{207}Pb/^{235}U	1σ	^{206}Pb/^{238}U	1σ	^{207}Pb/^{206}Pb	1σ	^{207}Pb/^{232}U	1σ	^{206}Pb/^{238}U	1σ
HL013-1																
01	335	74.4	1065	0.07	0.1232	0.0012	5.2084	0.0942	0.3065	0.0058	2003	16.7	1854	15.5	1724	28.5
02	393	146	219	0.66	0.2013	0.0023	14.5816	0.2237	0.5256	0.0068	2839	19.6	2788	14.7	2723	28.8
03	237	69.6	463	0.15	0.1252	0.0023	6.8243	0.0682	0.3843	0.0034	2031	33.2	2089	9.0	2097	15.8
04	200	46.9	428	0.11	0.1274	0.0054	7.7318	0.1678	0.3747	0.0059	2063	73.9	2200	19.6	2051	27.8
05	268	85.2	455	0.19	0.1700	0.0254	7.4894	0.2223	0.3714	0.0095	2558	252.8	2172	26.6	2036	44.7
06	318	106	204	0.52	0.2043	0.0023	15.4394	0.3552	0.5546	0.0126	2861	18.5	2843	22.0	2844	52.1
07	458	193	282	0.68	0.1909	0.0022	12.9641	0.2590	0.4987	0.0093	2750	18.7	2677	18.9	2608	40.2
08	463	188	225	0.83	0.2058	0.0024	14.8873	0.2646	0.5290	0.0077	2873	18.8	2808	17.0	2737	32.3
09	384	152	216	0.70	0.2016	0.0020	14.9464	0.2012	0.5421	0.0069	2839	12.0	2812	13.0	2792	28.8
10	276	60.2	852	0.07	0.1174	0.0035	5.1209	0.0698	0.2907	0.0040	1916	53.4	1840	11.7	1645	20.2
11	484	188	241	0.78	0.2016	0.0022	15.3508	0.2510	0.5548	0.0086	2839	17.6	2837	15.7	2845	35.6
12	308	108	178	0.61	0.1977	0.0039	14.8559	0.3142	0.5440	0.0092	2807	31.6	2806	20.2	2800	38.6
13	216	45.7	411	0.11	0.1388	0.0050	8.4047	0.2119	0.3897	0.0066	2213	63.0	2276	22.9	2121	30.5
14	290	97.6	438	0.22	0.1459	0.0030	7.5076	0.2235	0.3691	0.0054	2298	35.2	2174	26.7	2025	25.4
15	284	93.9	292	0.32	0.1737	0.0034	10.2376	0.2428	0.4253	0.0051	2594	33.3	2456	22.0	2284	23.3
16	238	60.6	608	0.10	0.1241	0.0011	6.0411	0.0759	0.3521	0.0040	2016	17.1	1982	11.0	1945	19.2
17	301	83.5	343	0.24	0.1697	0.0052	11.5946	0.4657	0.4635	0.0120	2555	50.9	2572	37.6	2455	53.1
18	366	121	404	0.30	0.1600	0.0021	9.1303	0.1548	0.4131	0.0066	2457	22.2	2351	15.6	2229	29.9
19	260	80.5	701	0.11	0.1243	0.0011	5.6617	0.0863	0.3291	0.0048	2020	15.9	1926	13.2	1834	23.5
20	269	54.8	940	0.06	0.1240	0.0010	5.1268	0.0755	0.2991	0.0045	2015	19.0	1841	12.6	1687	22.3
21	189	57.3	380	0.15	0.1488	0.0015	7.8009	0.1671	0.3781	0.0066	2332	17.7	2208	19.3	2067	31.1
22	388	157	228	0.69	0.2013	0.0016	14.9424	0.2192	0.5376	0.0076	2836	13.0	2812	14.1	2773	32.1
23	295	97.7	224	0.44	0.2003	0.0046	15.0850	0.5219	0.5379	0.0125	2829	37.0	2821	33.0	2775	52.5
24	405	54.6	932	0.06	0.1333	0.0046	4.5084	0.1059	0.2462	0.0068	2142	60.5	1733	19.6	1419	35.4
25	215	55.9	545	0.10	0.1276	0.0024	6.1954	0.0805	0.3522	0.0038	2065	33.2	2004	11.4	1945	18.3
26	253	41.3	678	0.06	0.1260	0.0012	6.5807	0.1256	0.3795	0.0081	2043	15.6	2057	16.9	2074	37.7
27	361	65.4	1077	0.06	0.1306	0.0012	5.0826	0.1141	0.2819	0.0065	2105	10.6	1833	19.1	1601	32.9
28	297	103	669	0.15	0.1221	0.0042	5.5767	0.1774	0.3289	0.0106	1987	61.1	1913	27.4	1833	51.4
29	271	64.2	656	0.10	0.1243	0.0026	6.4502	0.1047	0.3738	0.0058	2018	36.7	2039	14.3	2047	27.4
30	252	66.1	628	0.11	0.1243	0.0017	6.4651	0.1074	0.3750	0.0063	2020	24.4	2041	14.7	2053	29.4
31	326	107	448	0.24	0.1574	0.0043	9.7849	0.2225	0.4171	0.0080	2427	46.3	2415	21.0	2247	36.2
32	348	129	199	0.65	0.1965	0.0031	14.8533	0.3227	0.5433	0.0091	2797	30.6	2806	20.8	2797	38.1
33	509	212	233	0.91	0.2032	0.0025	15.4816	0.3219	0.5493	0.0108	2854	19.8	2845	19.9	2822	44.9
34	328	126	238	0.53	0.1899	0.0024	12.8136	0.3742	0.4864	0.0139	2743	20.7	2666	27.6	2555	60.1
35	205	72.3	121	0.60	0.1740	0.0102	15.1327	0.2584	0.5371	0.0098	2596	97.5	2824	16.4	2771	41.3
36	398	141	173	0.82	0.2079	0.0021	16.6554	0.2660	0.5793	0.0091	2900	16.4	2915	15.4	2946	37.1
HL013-2																
01	285	107	304	0.35	0.1488	0.0043	8.1073	0.2192	0.3910	0.0055	2332	49.7	2243	24.5	2127	25.5
02	222	40.8	358	0.11	0.1673	0.0037	10.6680	0.2221	0.4472	0.0074	2531	36.9	2495	19.4	2383	33.1
03	367	71.2	916	0.08	0.1227	0.0022	5.4034	0.0986	0.3203	0.0063	1995	32.6	1885	15.7	1791	31.0
04	332	57.5	373	0.15	0.2030	0.0032	15.8039	0.3306	0.5624	0.0081	2851	25.0	2865	20.1	2876	33.4
05	130.5	20.7	377	0.05	0.1249	0.0014	5.9637	0.0811	0.3463	0.0052	2028	20.1	1971	11.9	1917	25.1
06	403	140	223	0.63	0.1906	0.0022	13.7459	0.2271	0.5224	0.0090	2747	18.5	2732	15.7	2709	38.3
07	340	124	185	0.67	0.1916	0.0037	14.1755	0.2457	0.5368	0.0086	2767	32.1	2762	16.5	2770	36.2
08	225	45.1	607	0.07	0.1227	0.0013	6.2413	0.0728	0.3709	0.0047	1998	19.9	2010	10.3	2033	21.9

续表1

分析点号	含量/10^{-6}			Th/U	比值						年龄/Ma					
	Pb	Th	U		$^{207}Pb/^{206}Pb$	1σ	$^{207}Pb/^{235}U$	1σ	$^{206}Pb/^{238}U$	1σ	$^{207}Pb/^{206}Pb$	1σ	$^{207}Pb/^{232}U$	1σ	$^{206}Pb/^{238}U$	1σ
09	377	132	180	0.73	0.2041	0.0046	15.6436	0.2786	0.5620	0.0095	2859	30.7	2855	17.1	2875	39.2
10	301	112	134	0.84	0.2001	0.0058	15.1569	0.2429	0.5587	0.0086	2827	46.9	2825	15.4	2861	35.8
11	221	41.7	781	0.05	0.1259	0.0030	4.8253	0.0683	0.2738	0.0038	2043	8.2	1789	12.0	1560	19.1
12	177	35.4	474	0.07	0.1272	0.0028	6.3381	0.1148	0.3687	0.0050	2061	39.0	2024	15.9	2023	23.4
13	506	185	260	0.71	0.2068	0.0047	14.8576	0.2548	0.5359	0.0094	2881	37.0	2806	16.4	2766	39.6
14	436	140	351	0.40	0.2003	0.0041	12.8435	0.2030	0.4760	0.0060	2829	33.6	2668	15.0	2510	26.1
15	496	207	260	0.80	0.1970	0.0033	13.3346	0.1685	0.5031	0.0070	2802	27.8	2704	12.1	2627	30.2
16	230	70.2	163	0.43	0.1921	0.0064	14.8094	0.4647	0.5513	0.0132	2761	54.2	2803	29.9	2831	54.8
17	347	119	967	0.12	0.1406	0.0021	4.1282	0.1056	0.2172	0.0055	2235	25.8	1660	20.9	1267	28.9
18	311	115	194	0.59	0.2009	0.0029	14.6668	0.2007	0.5394	0.0080	2835	23.5	2794	13.1	2781	33.5
19	252	91	158	0.58	0.2111	0.0032	15.2951	0.3684	0.5317	0.0124	2914	19.3	2834	23.0	2749	52.4
20	292	118	318	0.37	0.1702	0.0035	9.3974	0.1770	0.4020	0.0061	2561	34.7	2378	17.4	2178	28.3
21	211	78.2	553	0.14	0.1250	0.0014	5.7494	0.0620	0.3358	0.0037	2029	20.2	1939	9.4	1866	17.9
22	218	93.1	440	0.21	0.1210	0.0068	5.5907	0.2258	0.3212	0.0106	1972	101.0	1915	34.8	1796	51.5
23	497	194	174	1.12	0.2097	0.0026	16.5251	0.1850	0.5725	0.0078	2903	20.8	2908	10.9	2918	32.0
24	188	58.9	401	0.15	0.1270	0.0041	6.4502	0.0997	0.3714	0.0060	2057	61.9	2039	13.7	2036	28.1
25	287	98.1	226	0.43	0.1991	0.0030	14.1961	0.2872	0.5151	0.0101	2820	24.4	2763	19.3	2678	42.8
26	277	98.2	157	0.63	0.2039	0.0026	15.6823	0.2101	0.5560	0.0075	2858	21.5	2858	12.9	2850	30.9
27	357	137	275	0.50	0.1662	0.0042	10.4822	0.1946	0.4281	0.0075	2520	42.9	2478	17.3	2297	33.9
28	556	184	388	0.48	0.2033	0.0023	14.9121	0.1865	0.5306	0.0071	2853	18.2	2810	12.1	2744	29.8
29	272	59.3	333	0.18	0.1921	0.0019	13.4273	0.2267	0.5043	0.0077	2761	16.4	2710	16.1	2632	32.8
30	406	161	286	0.56	0.1788	0.0038	11.7051	0.3395	0.4647	0.0126	2642	35.2	2581	27.2	2460	55.4
31	170	32.7	475	0.07	0.1185	0.0030	6.0298	0.0784	0.3680	0.0050	1944	44.8	1980	11.4	2020	23.6
HL005-3																
01	410	214	605	0.35	0.1932	0.0053	8.6984	0.1719	0.3153	0.0062	2769	44.8	2307	18.1	1767	30.2
02	346	135	364	0.37	0.1968	0.0051	11.6128	0.3150	0.4228	0.0103	2800	43.1	2574	25.4	2273	46.6
03	391	349	1285	0.27	0.1486	0.0088	2.8058	0.0666	0.1322	0.0030	2329	101.2	1357	17.8	801	17.0
04	424	210	271	0.78	0.2213	0.0028	17.6977	0.2181	0.5804	0.0074	2990	20.7	2973	12.0	2950	30.4
05	178	81	131	0.62	0.2116	0.0019	15.8690	0.2343	0.5432	0.0080	2918	14.5	2869	14.2	2797	33.4
06	361	153	547	0.28	0.2010	0.0020	11.2967	0.4545	0.4016	0.0145	2834	16.0	2548	37.6	2176	66.9
07	212	50	1287	0.04	0.1617	0.0017	2.9754	0.1087	0.1317	0.0039	2473	17.9	1401	27.8	797	22.3
08	287	180	1649	0.11	0.1377	0.0059	1.9925	0.0670	0.0978	0.0025	2199	74.1	1113	22.7	602	14.5
09	243	108	173	0.62	0.2125	0.0017	17.4082	0.1771	0.5936	0.0065	2925	13.4	2958	10.0	3004	26.5
10	278	160	1069	0.15	0.1697	0.0016	4.0166	0.0902	0.1711	0.0035	2555	17.1	1638	18.3	1018	19.1
11	178	93	111	0.84	0.2146	0.0015	17.4430	0.2786	0.5893	0.0099	2940	12.2	2960	15.5	2986	40.0
12	340	156	393	0.40	0.2029	0.0017	12.3310	0.3743	0.4383	0.0123	2850	14.4	2630	28.6	2343	55.2
13	500	323	629	0.51	0.1828	0.0072	9.7985	0.5673	0.3492	0.0178	2680	64.4	2416	53.4	1931	85.1
14	431	205	380	0.54	0.2041	0.0018	15.1691	0.3164	0.5384	0.0108	2859	9.1	2826	20.0	2777	45.4
15	288	87	346	0.25	0.2038	0.0020	11.2491	0.4784	0.4001	0.0167	2857	16.4	2544	39.7	2169	77.1
16	174	90	119	0.76	0.2060	0.0038	14.8461	0.2019	0.5220	0.0071	2876	25.0	2805	13.1	2708	30.1
17	454	342	1087	0.31	0.1864	0.0019	4.0160	0.0901	0.1558	0.0031	2711	17.3	1637	18.3	933	17.0
18	435	193	1416	0.14	0.1816	0.0014	5.0552	0.0814	0.2022	0.0036	2733	12.7	1829	13.7	1187	19.5
19	394	194	259	0.75	0.1957	0.0073	16.1690	0.1839	0.5628	0.0068	2790	61.1	2887	11.1	2878	28.3
20	429	109	1668	0.07	0.1661	0.0015	3.9993	0.0641	0.1743	0.0025	2520	47.2	1634	13.1	1036	13.8
21	347	73	1552	0.05	0.1711	0.0016	3.9542	0.0533	0.1674	0.0020	2568	14.7	1625	11.0	998	11.2
22	250	45	1417	0.03	0.1577	0.0013	2.5427	0.0408	0.1167	0.0017	2431	19.6	1284	11.7	712	9.8

续表1

分析点号	含量/10^{-6}			Th/U	比值						年龄/Ma					
	Pb	Th	U		$^{207}Pb/^{206}Pb$	1σ	$^{207}Pb/^{235}U$	1σ	$^{206}Pb/^{238}U$	1σ	$^{207}Pb/^{206}Pb$	1σ	$^{207}Pb/^{232}U$	1σ	$^{206}Pb/^{238}U$	1σ
23	523	107	1987	0.05	0.1755	0.0013	3.7849	0.0614	0.1562	0.0024	2611	17.1	1590	13.1	936	13.4
24	243	105	183	0.58	0.2098	0.0018	17.0611	0.2748	0.5904	0.0098	2906	13.6	2938	15.6	2991	39.9
25	366	174	307	0.57	0.2106	0.0013	15.1895	0.3000	0.5220	0.0098	2910	10.2	2827	18.9	2707	41.5
26	538	464	971	0.48	0.1914	0.0037	5.9320	0.2606	0.2211	0.0085	2754	30.4	1966	38.2	1288	44.7
27	478	149	1655	0.09	0.1729	0.0016	4.4863	0.0732	0.1881	0.0028	2586	14.7	1728	13.6	1111	15.4
28	513	234	389	0.60	0.2146	0.0017	17.1786	0.1983	0.5806	0.0063	2940	13.0	2945	11.3	2951	25.8
29	270	125	219	0.57	0.2097	0.0017	15.8007	0.1640	0.5467	0.0055	2903	8.2	2865	10.1	2812	23.0
30	232	99	180	0.55	0.2093	0.0037	16.7215	0.1586	0.5614	0.0057	2902	28.7	2919	9.3	2872	23.7
31	691	474	561	0.84	0.1978	0.0095	11.6275	0.2662	0.4219	0.0087	2809	78.4	2575	21.5	2269	39.5
32	164	76	113	0.67	0.2159	0.0018	17.5540	0.2688	0.5895	0.0086	2951	12.5	2966	14.8	2987	34.8
33	210	105	153	0.69	0.2144	0.0016	16.5313	0.1916	0.5589	0.0063	2939	11.7	2908	11.3	2862	26.3
34	157	74	112	0.66	0.2147	0.0019	16.8518	0.1780	0.5699	0.0063	2943	13.7	2926	10.3	2907	25.9
35	265	88	281	0.31	0.1999	0.0020	10.3242	0.4405	0.3630	0.0140	2826	16.7	2464	39.5	1996	66.3
36	637	243	3097	0.08	0.1648	0.0018	3.2910	0.0701	0.1441	0.0023	2505	18.8	1479	16.6	868	13.1
37	450	251	447	0.56	0.2032	0.0017	13.0130	0.3830	0.4622	0.0128	2854	13.6	2681	27.8	2449	56.6
38	141	64	130	0.49	0.2041	0.0017	14.0745	0.3131	0.4990	0.0106	2861	13.3	2755	21.2	2609	45.6
39	601	371	354	1.05	0.2122	0.0016	16.1421	0.1687	0.5514	0.0057	2924	12.0	2885	10.2	2831	23.8
40	216	144	330	0.44	0.1691	0.0093	7.5520	0.5075	0.2747	0.0183	2550	92.0	2179	60.3	1565	92.4
41	295	140	213	0.65	0.2132	0.0017	16.9258	0.1860	0.5752	0.0061	2931	13.0	2931	10.7	2929	25.1
42	394	149	1896	0.08	0.0963	0.0102	1.4874	0.0872	0.0764	0.0031	1554	201.4	925	35.6	474	18.8

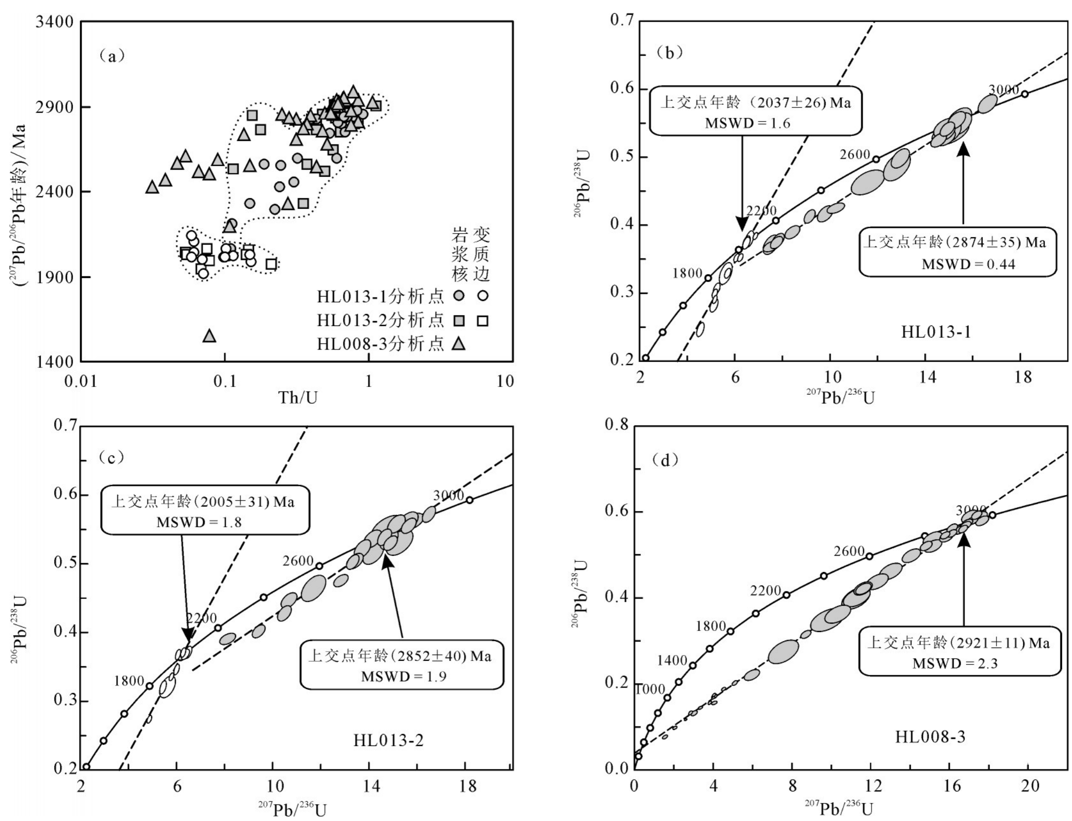

图4 黄陵片麻岩锆石测年Th/U−$^{207}Pb/^{206}Pb$年龄图(a)、HL013−1(b)、HL013−2(c)、HL005−3(d)谐和年龄图

Fig.4 Th/U−$^{207}Pb/^{206}Pb$ age diagram (a), U−Pb concordia diagrams(b, c, d) of the gneisses (HL013−1, HL013−2, HL005−3) from the Huangling area

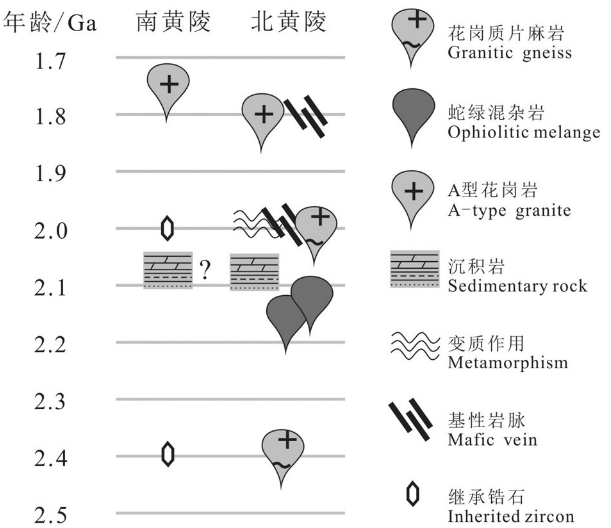

图5 南北黄陵古元古代构造岩浆事件对比图
（据Li et al., 2018）
Fig.5 Comparison chart of Paleoproterozoic tectono-magmatic events for north and south Huangling area
(after Li et al., 2018)

同碰撞花岗岩、变质作用、陆内伸展A型花岗岩和基性岩脉，对应古元古代复杂的洋陆转换过程。因此，笔者推测古元古代南黄陵、北黄陵西部与北黄陵中、东部可能处于不同的构造环境，经历了不同的演化过程。而南黄陵和北黄陵西部处于稳定地块环境，仅发育古元古代稳定沉积岩和1.76 Ga的A型花岗岩(Li et al., 2018)。

5.2 扬子陆块古元古代造山带

扬子陆块作为中国大陆的重要组成部分，对其古元古代造山带的研究及其与古元古代哥伦比亚超大陆的关系一直以来倍受关注(Zhao et al., 2004; Wu et al., 2012; Zhao et al., 2012; Dong et al., 2015; Han et al., 2017, 2018)。蛇绿混杂岩、岛弧岩浆岩、同碰撞花岗岩等是鉴别古老造山带最直接的标志(Dilek et al., 2011; Kusky et al., 2013; 张克信等, 2014)，黄陵地区发育完整的造山序列：2.15~2.12 Ga水月寺蛇绿岩(彭松柏等, 2016; Han et al., 2017, 2018)、2.0 Ga弧岩浆作用(Li et al., 2019)、2.0 Ga的同碰撞花岗岩(Li et al., 2014)，无疑代表古元古代造山带经过位置（图5）；Wu et al.(2012)曾报道后河杂岩中存在~2.1 Ga岛弧有关的花岗岩，湖北钟祥出露~2.0 Ga同碰撞I型花岗岩(Wang et al., 2015)，以及孝感金盆水库附近的~2.0 Ga同碰撞花岗岩（郭盼等, 2020），说明这些区域应同样是造山带的组成部分。追踪俯冲-造山过程产生的变质作用也是探索造山带的重要手段，扬子陆块典型太古宙建造包括陡岭杂岩(Hu et al., 2013；Wu et al., 2014)、鱼洞子杂岩(Hui et al., 2017)、崆岭杂岩(凌文黎等, 1999; Gao et al., 2011；Chen et al., 2013a; Guo et al., 2014, 2015；Li et al., 2016)、杨坡杂岩(Zhou et al., 2015；Wang et al., 2018)、黄土岭麻粒岩(Sun et al., 2008；Wu et al., 2008)。其中仅崆岭杂岩(Zhang et al., 2006；Wu et al., 2009；Gao et al., 2011；Yin et al., 2013；Chen et al., 2013a；邱啸飞等, 2017, 2019)和黄土岭麻粒岩(Sun et al., 2008；Wu et al., 2008)记录了~2.0 Ga的变质事件，并在桐柏地区凤凰咀、武胜关高级变质岩中也获得了该变质年龄(胡娟等, 2012)，说明~2.0 Ga变质作用主要发育于黄陵、桐柏—大别地区。另外，扬子陆块白马尖、宁乡、板溪、镇远等地曾获得2.0 Ga左右的捕获锆石、碎屑锆石(Bryant et al., 2004; Zheng et al., 2006; Wang et al., 2012) ，为这些位置存在~2.0 Ga的构造-岩浆作用提供了间接证据。

此外，造山后伸展的一套裂谷火山-沉积岩、A型花岗岩、基性岩脉组合也是追踪古老造山带位置及与超大陆关系的有效线索，而扬子西、北缘广泛出露古元古代末—中元古代初伸展环境的岩石组合。汉南后河(邓奇等, 2017)、黄陵圈椅埫(Xiong et al., 2009; Peng et al., 2012b)、钟祥华山观(Zhou et al., 2017)、董岭(Chen et al., 2016)等地均发育~1.8 Ga的A型花岗岩，崆岭杂岩(赵敏, 2013)、鱼洞子杂岩(Hui et al., 2017)均被~1.8 Ga的伸展型基性岩脉侵位，说明它们均卷入了古元古代造山后的伸展作用。另扬子西缘1.70~1.66 Ga河口群(Chen et al., 2013b)、东川群(Zhao et al., 2010b)、大红山群(Wang et al., 2014)及其中近同期的基性岩脉也代表一套裂谷建造，其形成时间较扬子北缘伸展型岩体、岩脉略晚，Wang et al. (2014)根据这一特征认为华南在哥伦比亚超大陆中与北美、澳大利亚相连。

根据前人研究不难发现，古元古代与造山带相关的岩石建造主要出露于扬子北缘，据此Wang et al.(2015)提出沿着后河、黄陵、冷水、黄土岭等地发育古元古代造山带（图6中①），华南位于哥伦比亚

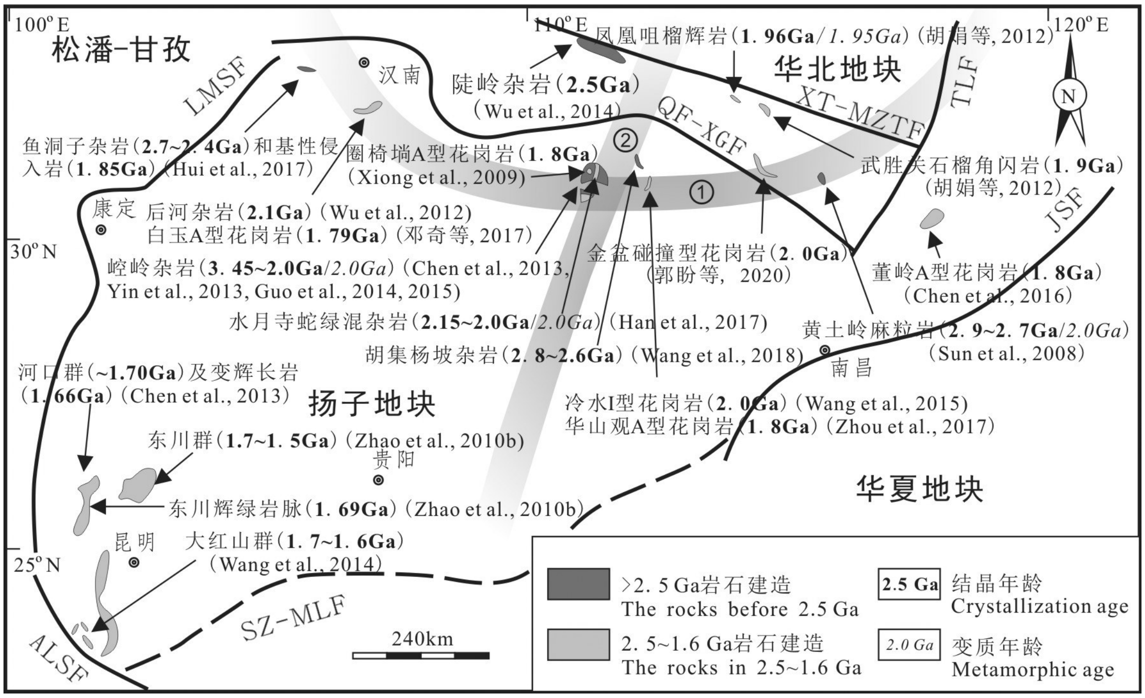

图6 扬子陆块>1.6Ga岩石分布示意图(据Li et al., 2019修改)

①—Wang et al.(2015)推测古元古代造山带位置;②—李一鹤(2016)推测古元古代造山带位置;XT-MZTF—晓天—磨子潭断裂;QF-XGF—青峰—襄广断裂;TLF—郯庐断裂;LMSF—龙门山断裂;ALSF—哀牢山断裂;SZ-MLF—师宗—弥勒断裂;JSF—江绍断裂

Fig.6 Distribution diagram of the >1.6 Ga rocks in Yangtze block (modified from Li et al., 2019)

①-Supposed Poleoproterozoic orogenic belt of Wang et al., 2015; ②-Supposed Poleoproterozoic orogenic belt of Li Yihe, 2016; XT-MZTF-Xiaotian- Mozitan fault belt; QF-XGF-Qingfeng-Xiangguang fault belt; TLF-Tanlu fault belt; LMSF-Longmen Mountain fault belt; ALSF-Ailao Mountain fault belt; SZ-MLF-Shizong- Mile fault belt; JSF-Jiangshao fault belt

超大陆西北角与非洲南部、澳大利亚相连。而另有学者根据古元古代水月寺蛇绿混杂岩南北展布特点,并结合扬子东西部碎屑锆石、捕获锆石年龄信息、地球物理资料等,提出扬子中部存在北东向古元古代造山带(Dong et al., 2015; Li et al., 2016; 李一鹤, 2016),并认为在哥伦比亚超大陆形成过程中,扬子东、西部微陆块和澳大利亚西部2个、非洲东南部2个微陆块之间发生了重组(李一鹤, 2016)。早期大陆形成以微陆块之间的拼合为主,中国大陆新太古代、新元古代均曾出现多块体拼贴的演化模式(Li et al., 2008; 陆松年等, 2016)。根据扬子陆块2.1~1.6 Ga构造-岩浆分布特点,推测古元古代扬子陆块存在多条不同方向、不同规模的造山带,扬子陆块古元古代可能同样具有多块体拼贴的演化特征,但现有的证据暂时无法准确揭示扬子古元古代造山带的数量、方向及范围。而广泛发育2.1~1.6 Ga的构造岩浆活动,一定程度上说明扬子陆块可能与哥伦比亚超大陆的形成过程有关。

6 结 论

(1)北黄陵太古代—古元古代片麻岩、表壳岩中广泛记录了~2.0 Ga的变质事件,而南黄陵类似建造中均未获得该变质年龄,这是南北黄陵古元古代最重要的差异,说明二者在古元古代可能属于不同地块或者同一地块不同部位,经历了不同的地质演化过程。

(2)大量的证据揭示,扬子陆块古元古代可能存在多条不同方向、不同规模的造山带,其古元古代可能具有多块体拼贴的演化特征,但具体的造山带数量、方向及范围需要进一步研究,而广泛发育2.1~1.6 Ga的构造岩浆活动记录说明扬子陆块可能与哥伦比亚超大陆形成过程有关。

致谢:南京宏创地质勘查技术服务有限公司对锆石挑选、制靶、反射光、透射光和阴极发光拍照提供帮助,湖北省地质试验测试中心对锆石LA-ICP-MS测试提供技术指导,成都地质调查中心邹光富研究员和

匿名审稿人提出大量修改意见,对文章质量的提升起了较大作用,在此一致表达谢意。

注释

❶湖北省地质调查院. 2005. 荆门市幅H49C001003 1:25万区域地质调查报告[R]. 武汉: 湖北省地质调查院.

❷湖北省地质调查院. 2007. 建始县幅H49C002002 1:25万区域地质调查报告[R]. 武汉: 湖北省地质调查院.

References

Bryant Derek L, Ayers John C, Gao Shan, Miller Calvin F, Zhang Hongfei. 2004. Geochemical, age, and isotopic constraints on the location of the Sino−Korean/Yangtze Suture and evolution of the Northern Dabie Complex, East Central China[J]. Geological Society of America, 116(5/6): 698−717.

Chen Kang, Gao Shan, Wu Yuanbao, Guo Jingliang, Hu Zhaochu, Liu Yongsheng, Zong Keqing, Liang Zhengwei, Geng Xianlei. 2013a. 2.6−2.7 Ga crustal growth in Yangtze craton, South China[J]. Precambrian Research, 224: 472−490.

Chen Wei Terry, Zhou Meifu, Zhao Xinfu. 2013b. Late Paleoproterozoic sedimentary and mafic rocks in the Hekou area, SW China: Implication for the reconstruction of the Yangtze Block in Columbia[J]. Precambrian Research, 231: 61−77.

Chen Zhihong, Xing Guangfu. 2016. Geochemical and zircon U−Pb−Hf−O isotopic evidence for a coherent Paleoproterozoic basement beneath the Yangtze Block, South China[J]. Precambrian Research, 279: 81−90.

Deng Hao, Peng Songbai, Polat Ali, Kusky Timothy, Jiang Xingfu, Han Qingsen, Wang Lu, Huang Yang, Wang Junpeng, Zeng Wen, Hu Zhengxiang. 2017. Neoproterozoic IAT intrusion into Mesoproterozoic MOR Miaowan Ophiolite, Yangtze Craton: Evidence for evolving tectonic settings[J]. Precambrian Research, 289: 75−94.

Deng Qi, Wang Zhengjiang, Wang Jian, Cui Xiaozhuang, Ma Long, Xiong Xiaohui. 2017. Discovery of the Baiyu ~1.79 Ga A−type granite in the Beiba area of the northwestern margin of Yangtze Block: Constraints on tectonic evolution of South China[J]. Acta Geol. Sinica, 91(7): 1454−1466(in Chinese with English abstract).

Dilek Y, Furnes H. 2011. Ophiolite genesis and global tectonics: Geochemical and tectonic fingerprinting of ancient oceanic lithosphere[J]. Geological Society of America Bulletin, 123(3/4): 387−411.

Dong S W, Zhang Y Q, Gao R, Su J B, Liu M, Li J H. 2015. A possible buried Paleoproterozoic collisional orogen beneath central South China: Evidence from seismic−reflection profiling[J]. Precambrian Research, 264: 1−10.

Gao S, Yang J, Zhou L, Li M, Hu Z, Guo J, Yuan H, Gong H, Xiao G, Wei J. 2011. Age and growth of the Archean Kongling terrain, South China, with emphasis on 3.3 Ga granitoid gneisses[J]. American Journal of Science, 311(2): 153−182.

Gao Shan, Qiu Yumin, Ling Wenli, McNaughton Neal J., Groves David I. 2001. SHRIMP single zircon U−Pb dating of the Kongling high−grade metamorphic terrain: Evidence for >3.2 Ga old continental crust in the Yangtze Craton[J]. Sci. China, Ser. D Earth Sci., 31(1): 27−35(in Chinese).

Guo Jingliang, Gao Shan, Wu Yuanbao, Li Ming, Chen Kang, Hu Zhaochu, Liang Zhengwei, Liu Yongsheng, Zhou Lian, Zong Keqing, Zhang Wen, Chen Haihong. 2014. 3.45 Ga granitic gneisses from the Yangtze Craton, South China: Implications for Early Archean crustal growth[J]. Precambrian Research, 242: 82−95.

Guo Jingliang, Wu Yuanbao, Gao Shan, Jin Zhenmin, Zong Keqing, Hu Zhaochu, Chen Kang, Chen Haihong, Liu Yongsheng. 2015. Episodic Paleoarchean−Paleoproterozoic (3.3−2.0 Ga) granitoid magmatism in Yangtze Craton, South China: Implications for Late Archean tectonics[J]. Precambrian Research, 270: 246−266.

Han Qingsen, Peng Songbai, Kusky Timothy, Polat Ali, Jiang Xingfu, Cen Yang, Liu Songfeng, Deng Hao. 2017. A Paleoproterozoic ophiolitic mélange, Yangtze craton, South China: Evidence for Paleoproterozoic suturing and microcontinent amalgamation[J]. Precambrian Research, 293: 13−38.

Han Qingsen, Peng Songbai, Polat Ali, Kusky Timothy, Deng Hao, Wu Tuoyu. 2018. A ca.2.1 Ga Andean−type margin built on metasomatized lithosphere in the northern Yangtze craton, China: Evidence from high−Mg basalts and andesites[J]. Precambrian Research, 309: 309−324.

Hu Juan, Liu Xiaochun, Chen Longyao, Qu Wei, Li Huaikun, Geng Jianzhen. 2013. A ~2.5 Ga magmatic event at the northern margin of the Yangtze craton: Evidence from U−Pb dating and Hf isotope analysis of zircons from the Douling Complex in the South Qinling orogen[J]. Chinese Science Bulletin, 58(28/29): 3564−3579.

Hu Juan, Liu Xiaochun, Qu Wei, Cui Jianjun. 2012. Zircon U−Pb Ages of Paleoproterozoic Metabasites from the Tongbai Orogen and Their Geological Significance[J]. Acta Geoscientica Sinica, 33(3): 305−315(in Chinese with English abstract).

Hui Bo, Dong Yunpeng, Cheng Chao, Long Xiaoping, Liu Xiaoming, Yang Zhao, Sun Shengsi, Zhang Feifei, Varga Jan. 2017. Zircon U−Pb chronology, Hf isotope analysis and whole−rock geochemistry for the Neoarchean−Paleoproterozoic Yudongzi complex, northwestern margin of the Yangtze craton, China[J]. Precambrian Research, 301: 65−85.

Jiang Xingfu, Peng Songbai, Kusky Timothy M, Wang Lu, Wang Junpeng, Deng Hao. 2012. Geological features and deformational ages of the basal thrust belt of the miaowan ophiolite in the southern Huangling anticline and its tectonic implications[J]. Journal of Earth Science, 23(5): 705−718.

Jiang Xingfu, Peng Songbai, Polat Ali, Kusky Timothy, Wang Lu, Wu

Tuoyu, Lin Musen, Han Qingsen. 2016. Geochemistry and geochronology of mylonitic metasedimentary rocks associated with the Proterozoic Miaowan Ophiolite Complex, Yangtze craton, China: Implications for geodynamic events[J]. Precambrian Research, 279: 37−56.

Jiao Wenfang, Wu Yuanbao, Yang Saihong, Peng Min, Wang Jing. 2009. The oldest basement rock in the Yangtze Craton revealed by zircon U−Pb age and Hf isotope composition[J]. Science in China Series D: Earth Sciences, 52: 1393−1399.

Kusky T M, Windley B F, Safonova I, Wakita K, Wakabayashi J, Polat A, Santosh M. 2013. Recognition of ocean plate stratigraphy in accretionary orogens through Earth history: A record of 3.8 billion years of sea floor spreading, subduction, and accretion[J]. Gondwana Research, 24(2): 501−547.

Li Longming, Lin Shoufa, Davis Donald W, Xiao Wenjiao, Xing Guangfu, Yin Changqing. 2014. Geochronology and geochemistry of igneous rocks from the Kongling terrane: Implications for Mesoarchean to Paleoproterozoic crustal evolution of the Yangtze Block[J]. Precambrian Research, 255: 30−47.

Li Qiwei, Zhao Junhong, Wang Wei. 2019. Ca. 2.0 Ga mafic dikes in the Kongling Complex, South China: Implications for the reconstruction of Columbia[J]. Journal of Asian Earth Sciences, 169: 323−335.

Li Yihe, Li Xiyao, Zheng Jianping, Xiong Qing, Wang Wei, Ping Xianquan, Tang Huayun. 2016. Petrogenesis and tectonic implications of Paleoproterozoic metapelitic rocks in the Archean Kongling Complex from the northern Yangtze Craton, South China[J]. Precambrian Research, 276: 158−177.

Li Yihe, Zheng Jianping, Ping Xianquan, Xiong Qing, Xiang Lu, Zhang Hui. 2018. Complex growth and reworking processes in the Yangtze cratonic nucleus[J]. Precambrian Research, 311: 262−277.

Li Yihe. 2016. Crust Evolutional Process of Yangtze Craton during Archean−Paleoproterozoic Period[D]. Wuhan: China University of Geosciences(Wuhan)(in Chinese with English abstract).

Li Z X, Bogdanova S V, Collins A S, Davidson A, De Waele B, Ernst R E, Fitzsimons I C W, Fuck R A, Gladkochub D P, Jacobs J, Karlstrom K E, Lu S, Natapov L M, Pease V, Pisarevsky S A, Thrane K, Vernikovsky V. 2008. Assembly, configuration, and break− up history of Rodinia: A synthesis[J]. Precambrian Research, 160(1/2): 179−210.

Ling Wenli, Cheng Jianping, Gao Shan, Zhang Benren, Luo Tingchuan. 1999. Geochemical features of Neoarchean continental crust and mantle in China: Correlation among Yangtze Kongling, North China Craton and Dabie Orogenic Belt[J]. Earth Science, 24 (3): 25−30(in Chinese with English abstract).

Ling Wenli, Gao Shan, Cheng Jianping, Jiang Linsheng, Yuan Honglin, Hu Zhaochu. 2006. Neoproterozoic magmatic events within the Yangtze continental interior and along its northern margin and their tectonic implication: Constraint from the ELA− ICPMS U− Pb geochronology of zircons from the Huangling and Hannan complexes[J]. Acta Petrologica Sinica, 22(2): 387−396(in Chinese with English abstract).

Liu Yongsheng, Gao Shan, Hu Zhaochu, Gao Changgui, Zong Keqing, Wang Dongbing. 2009. Continental and oceanic crust recycling−induced melt− peridotite interactions in the Trans− North China Orogen: U− Pb dating, Hf isotopes and trace elements in zircons from mantle xenoliths[J]. Journal of Petrology, 51(1/2): 537−571.

Lu Songnian, Wang Huichu, Hao Guojie, Xiang Zhenqun. 2016. The debate concerning the beginning of the plate tectonics[J]. Geology in China, 43(3): 709−720(in Chinese with English abstract).

Ludwig Kenneth R. 2003 User's Manual for Isoplot 3.00: A Geochronological Toolkit for Microsoft Excel[M]. Berkeley: Berkeley Geochronology Center.

Peng Min, Wu Yuanbao, Gao Shan, Zhang Hongfei, Wang Jing, Liu Xiaochi, Liu Yongsheng, Gong Hujun, Zhou Lian, Hu Zhaochu, Yuan Honglin. 2012b. Geochemistry, zircon U− Pb age and Hf isotope compositions of Paleoproterozoic aluminous A− type granites from the Kongling terrain, Yangtze Block: Constraints on petrogenesis and geologic implications[J]. Gondwana Research, 22 (1): 140−151.

Peng Songbai, Han Qingsen, Ali P, Kusky T M. 2016. Discovery of the Paleoproterozoic ophiolitic melange in the northern Huangling dome, Yangtze Craton[J]. Earth Science, 41(12): 2117− 2118 (in Chinese with English Abstract).

Peng Songbai, Kusky T M, Jiang X F, Wang L, Wang J P, Deng H. 2012a. Geology, geochemistry, and geochronology of the Miaowan ophiolite, Yangtze craton: Implications for South China's amalgamation history with the Rodinian supercontinent[J]. Gondwana Research, 21(2/3): 577−594.

Peng Songbai, Li Changnian, Kusky Timothy M, Wang Lu, Zhang Xianjin, Jiang Xingfu, Xiong Chengren. 2010. Discovery and its tectonic significance of the Proterozoic Miaowan ophiolites in the southern Huangling anticline,western Hubei,China[J]. Geological Bulletin of China, 29(1): 8−20(in Chinese with English abstract).

Qiu Xiaofei, Yang Hongmei, Lu Shansong, Zhang Liguo, Duan Ruichun, Du Guomin. 2016. Geochronology of the Khondalite aeries in the Kongling Complex, Yangtze Craton and its geological implication[J]. Geotectonica et Metallogenia, 40(3): 549− 558(in Chinese with English abstract).

Qiu Xiaofei, Yang Hongmei, Zhao Xiaoming, Lu Shansong, Jiang Tuo, Duan Ruichun, Liu Zhongpeng, Peng Lianhong, Wei Yunxu. 2019. The Neoarchean granitic gneisses in the Kongling Complex, Yangtze Craton: Petrogenesis and tectonic implications[J]. Earth Science, 44(2): 415−426(in Chinese with English abstract).

Qiu Xiaofei, Zhao Xiaoming, Yang Hongmei, Wei Yunxu, Wu Nianwen, Lu Shansong, Jiang Tuo, Peng Lianhong. 2017. Paleoproterozoic metamorphic event in the nucleus of the Yangtze craton: Evidence from U−Pb geochronology of the metamorphic zircons from the khondalite[J]. Geological Bulletin of China, 36(5): 706−714(in Chinese with English abstract).

Qiu Yumin M, Gao Shan, McNaughton Neal J, Groves David I, Ling Wenli. 2000. First evidence of >3.2 Ga continental crust in the Yangtze craton of south China and its implications for Archean crustal evolution and Phanerozoic tectonics[J]. Geology, 28(1): 11.

Sun M, Chen N, Zhao G, Wilde S A, Ye K, Guo J, Chen Y, Yuan C. 2008. U−Pb Zircon and Sm−Nd isotopic study of the huangtuling granulite, Dabie−Sulu belt, China: Implication for the Paleoproterozoic tectonic history of the yangtze craton[J]. American Journal of Science, 308(4): 469−483.

Wang Wei, Zhou Meifu, Zhao Xinfu, Chen Wei Terry, Yan Danping. 2014. Late Paleoproterozoic to Mesoproterozoic rift successions in SW China: Implication for the Yangtze Block− North Australia− Northwest Laurentia connection in the Columbia supercontinent[J]. Sedimentary Geology, 309: 33−47.

Wang Xiaolei, Shu Liangshu, Xing Guangfu, Zhou Jincheng, Tang Ming, Shu Xujie, Qi Liang, Hu Yanhua. 2012. Post− orogenic extension in the eastern part of the Jiangnan orogen: Evidence from ca 800− 760 Ma volcanic rocks[J]. Precambrian Research, 222− 223: 404−423.

Wang Zhengjiang, Deng Qi, Duan Taizhong, Yang Fei, Du Qiuding, Xiong Xiaohui, Liu Hao, Cao Bofeng. 2018. 2.85 Ga and 2.73 Ga A− type granites and 2.75 Ga trondhjemite from the Zhongxiang Terrain: Implications for early crustal evolution of the Yangtze Craton, South China[J]. Gondwana Research, 61: 1−19.

Wang Zhengjiang, Wang Jian, Deng Qi, Du Qiuding, Zhou Xiaolin, Yang Fei, Liu Hao. 2015. Paleoproterozoic I− type granites and their implications for the Yangtze block position in the Columbia supercontinent: Evidence from the Lengshui Complex, South China[J]. Precambrian Research, 263: 157−173.

Wei Junqi, Wang Jianxiong. 2012. Zircon Age and Hf Isotope Compositions of Amphibolite Enclaves from the Kongling Complex[J]. Geological Journal of China Universities, 18(4): 589−600(in Chinese with English abstract).

Wei Yunxu, Peng Songbai, Jiang Xingfu, Peng Zhongqin, Peng Lianhong, Li Zhihong, Zhou Peng, Zeng Xiongwei. 2012. SHRIMP zircon U−Pb ages and geochemical characteristics of the neoproterozoic granitoids in the Huangling anticline and its tectonic setting[J]. Journal of Earth Science, 23(5): 659−676.

Wu Hui, Zhang Yinghua, Ling Wenli, Bai Xiao, Ma Qian, Berkana Wafa, Cheng Jianping, Peng Lianhong. 2016. Recognition of mantle input and its tectonic implication for the nature of ~815 Ma magmatism in the Yangtze continental interior, South China[J]. Precambrian Research, 279: 17−36.

Wu Y B, Gao S, Gong H J, Xiang H, Jiao W F, Yang S H, Liu Y S, Yuan H L. 2009. Zircon U−Pb age, trace element and Hf isotope composition of Kongling terrane in the Yangtze Craton: Refining the timing of Palaeoproterozoic high− grade metamorphism[J]. Journal of Metamorphic Geology, 27(6): 461−477.

Wu Yuanbao, Gao Shan, Zhang Hongfei, Zheng Jianping, Liu Xiaochi, Wang Hao, Gong Hujun, Zhou Lian, Yuan Honglin. 2012. Geochemistry and zircon U−Pb geochronology of Paleoproterozoic arc related granitoid in the Northwestern Yangtze Block and its geological implications[J]. Precambrian Research, 200− 203: 26−37.

Wu Yuanbao, Zheng Yongfei, Gao Shan, Jiao Wenfang, Liu Yongsheng. 2008. Zircon U−Pb age and trace element evidence for Paleoproterozoic granulite− facies metamorphism and Archean crustal rocks in the Dabie Orogen[J]. Lithos, 101(3/4): 308−322.

Wu Yuanbao, Zhou Guangyan, Gao Shan, Liu Xiaochun, Qin Zhengwei, Wang Hao, Yang Jianzhou, Yang Saihong. 2014. Petrogenesis of Neoarchean TTG rocks in the Yangtze Craton and its implication for the formation of Archean TTGs[J]. Precambrian Research, 254: 73−86.

Xiong Qing, Zheng Jianping, Yu Chunmei, Su Yuping, Tang Huayun, Zhang Zhihai. 2009. Zircon U−Pb age and Hf isotope of Quanyishang A− type granite in Yichang: Signification for the Yangtze continental cratonization in Paleoproterozoic[J]. Science Bulletin, 54(3): 436−446.

Yin Changqing, Lin Shoufa, Davis Donald W, Zhao Guochun, Xiao Wenjiao, Li Longming, He Yanhong. 2013. 2.1− 1.85 Ga tectonic events in the Yangtze Block, South China: Petrological and geochronological evidence from the Kongling Complex and implications for the reconstruction of supercontinent Columbia[J]. Lithos, 182−183: 200−210.

Zhang Kexin, Feng Qinglai, Song Bowen, Zhang Zhiyong, Wang Yonghe, Pan Guitang, Lu Songnian, Zhao Xiaoming, Xing Guangfu. 2014. Non− Smithian strata in the orogen[J]. Earth Science Frontiers, 21(2): 36−47(in Chinese with English abstract).

Zhang Shaobing, Zheng Yongfei, Wu Yuanbao, Zhao Zifu, Gao Shan, Wu Fuyuan. 2006. Zircon U− Pb age and Hf− O isotope evidence for Paleoproterozoic metamorphic event in South China[J]. Precambrian Research, 151(3/4): 265−288.

Zhang Shaobing, Zheng Yongfei, Zhao Zifu, Wu Yuanbao, Yuan Honglin, Wu Fuyuan. 2009. Origin of TTG− like rocks from anatexis of ancient lower crust: Geochemical evidence from Neoproterozoic granitoids in South China[J]. Lithos, 113(3/4): 347−368.

Zhao Guochun, Cawood Peter A. 2012. Precambrian geology of China[J]. Precambrian Research, 222−223: 13−54.

Zhao Guochun, Sun Min, Wilde Simon A., Li Sanzhong. 2004. A Paleo− Mesoproterozoic supercontinent: assembly, growth and breakup[J]. Earth−Science Reviews, 67(1/2): 91−123.

Zhao Junhong, Zhou Meifu, Zheng Jianping. 2010a. Metasomatic mantle source and crustal contamination for the formation of the Neoproterozoic mafic dike swarm in the northern Yangtze Block, South China[J]. Lithos, 115(1/4): 177−189.

Zhao Junhong, Zhou Meifu, Zheng Jianping. 2013. Neoproterozoic high−K granites produced by melting of newly formed mafic crust in the Huangling region, South China[J]. Precambrian Research, 233: 93−107.

Zhao Min. 2013. Huangling Mafic Crystalline Basement−Zircon Age and Significance of Ultramafic Rocks[D]. Xi'an: Northwest University(in Chinese with English abstract).

Zhao Xinfu, Zhou Meifu, Li Jianwei, Sun Min, Gao Jianfeng, Sun Weihua, Yang Jinhui. 2010b. Late Paleoproterozoic to early Mesoproterozoic Dongchuan Group in Yunnan, SW China: Implications for tectonic evolution of the Yangtze Block[J]. Precambrian Research, 182(1/2): 57−69.

Zheng Y F, Zhao Z F, Wu Y B, Gong B. 2006. Protolith nature of deeply subducted continent: Zircon U−Pb age, Hf and O isotope constraints from UHP eclogite and gneiss in the Dabie orogen[J]. Geochimica et Cosmochimica Acta, 70(18, Supplement): A745.

Zhou Guangyan, Wu Yuanbao, Gao Shan, Yang Jianzhou, Zheng Jianping, Qin Zhengwei, Wang Hao, Yang Saihong. 2015. The 2.65 Ga A−type granite in the northeastern Yangtze craton: Petrogenesis and geological implications[J]. Precambrian Research, 258: 247−259.

Zhou Guangyan, Wu Yuanbao, Wang Hao, Qin Zhengwei, Zhang Wenxiang, Zheng Jianping, Yang Saihong. 2017. Petrogenesis of the Huashanguan A−type granite complex and its implications for the early evolution of the Yangtze Block[J]. Precambrian Research, 292: 57−74.

Zhou Liangliang, Wei Junqi, Wang Fang, Chou Xiumei. 2017. Optimizationof the Working Parameters of LA−ICP−MS and Its Application to Zircon U−Pb Dating[J]. Rock and Mineral Analysis, 36(4): 350−359(in Chinese with English abstract).

附中文参考文献

邓奇, 汪正江, 王剑, 崔晓庄, 马龙, 熊小辉. 2017. 扬子地块西北缘碑坝地区白玉~1.79 Ga A型花岗岩的发现及其对构造演化的制约[J]. 地质学报, 91(7): 1454−1466.

高山, Qiu Yumin, 凌文黎, McNaughton Neal J., Groves David I. 2001. 崆岭高级变质地体单颗粒锆石SHRIMP U—Pb年代学研究——扬子克拉通>3.2 Ga陆壳物质的发现[J]. 中国科学:D辑, 31(1): 27−35.

郭盼, 陈超, 吴波, 陈小龙, 孔令耀, 刘成新. 西大别 ~ 2.0 Ga变质花岗岩的发现及其Hf同位素特征[J/OL]. 中国地质: 1−18 [2020−06−23]. http://kns.cnki.ne t/ kcms / detail / 11. 1167. P. 20200304. 1649.004.html.

胡娟, 刘晓春, 曲玮, 崔建军. 2012. 桐柏造山带古元古代变质基性岩的锆石U−Pb年龄及其地质意义[J]. 地球学报, 33(3): 305−315.

李一鹤. 2016. 扬子克拉通太古宙至古元古代地壳演化过程研究[D]. 武汉: 中国地质大学(武汉).

凌文黎, 程建萍, 高山, 张本仁, 骆庭川. 1999. 扬子崆岭新太古代壳−幔地球化学特征及其与华北克拉通、大别造山带的对比[J]. 地球科学, 24(3): 25−30.

凌文黎, 高山, 程建萍, 江麟生, 袁洪林, 胡兆初. 2006. 扬子陆核与陆缘新元古代岩浆事件对比及其构造意义——来自黄陵和汉南侵入杂岩ELA−ICPMS锆石U−Pb同位素年代学的约束[J]. 岩石学报, 22(2): 387−396.

陆松年, 王惠初, 郝国杰, 相振群. 2016. 关于板块运动启动时间的争论[J]. 中国地质, 43(3): 709−720.

彭松柏, 韩庆森, Ali Polat, Kusky Timothy M. 2016. 扬子克拉通黄陵穹隆北部发现古元古代蛇绿混杂岩[J]. 地球科学, 41(12): 2117−2118.

彭松柏, 李昌年, Kusky Timothy M, 王璐, 张先进, 蒋幸福, 熊承仁. 2010. 鄂西黄陵背斜南部元古宙庙湾蛇绿岩的发现及其构造意义[J]. 地质通报, 29(1): 8−20.

邱啸飞, 杨红梅, 卢山松, 张利国, 段瑞春, 杜国民. 2016. 扬子克拉通崆岭杂岩孔兹岩系同位素年代学研究及其地质意义[J]. 大地构造与成矿学, 40(3): 549−558.

邱啸飞, 杨红梅, 赵小明, 卢山松, 江拓, 段瑞春, 刘重芃, 彭练红, 魏运许. 2019. 扬子克拉通崆岭杂岩新太古代花岗片麻岩成因及其构造意义[J]. 地球科学, 44(2): 415−426.

邱啸飞, 赵小明, 杨红梅, 魏运许, 吴年文, 卢山松, 江拓, 彭练红. 2017. 扬子陆核古元古代变质事件——来自孔兹岩系变质锆石U−Pb同位素年龄的证据[J]. 地质通报, 36(5): 706−714.

魏君奇, 王建雄. 2012. 崆岭杂岩中斜长角闪岩包体的锆石年龄和Hf同位素组成[J]. 高校地质学报, 18(4): 589−600.

张克信, 冯庆来, 宋博文, 张智勇, 王永和, 潘桂棠, 陆松年, 赵小明, 邢光福. 2014. 造山带非史密斯地层[J]. 地学前缘, 21(2): 36−47.

赵敏. 2013. 黄陵结晶基底中镁铁—超镁铁岩的锆石年龄及意义[D]. 西安: 西北大学.

周亮亮, 魏均启, 王芳, 仇秀梅. 2017. LA−ICP−MS工作参数优化及在锆石U−Pb定年分析中的应用[J]. 岩矿测试, 36(4): 350−359.